PCCP

PAPER

View Article Online
View Journal | View Issue

Check for updates

Cite this: *Phys. Chem. Chem. Phys.*, 2024, **26**, 18129

Thermally activated delayed fluorescence emitters for efficient sensitization of europium(III)†

Neena K. Kalluvettukuzhy, Michal R. Maciejczyk and Neil Robertson *

Received 19th April 2024,
Accepted 30th May 2024

DOI: 10.1039/d4cp01610f

rsc.li/pccp

We demonstrate for the first time a unique approach to efficiently sensitize lanthanides(III) using photosensitizer ligands that show thermally activated delayed fluorescence (TADF). TADF ligands have very small singlet (S_1) and triplet (T_1) excited state energy splitting and S_1/T_1 energy levels are in optimum energy to the acceptor level of Eu(III) to enable high energy transfer efficiency. The synthesized Eu(III) coordination polymers with TADF ligands showed bright red luminescence with an outstanding sensitization efficiency of 90–94% and Φ_{tot} of 79–85% in poly(methyl methacrylate) encapsulated films. This rational approach of efficiently sensitizing lanthanides with TADF ligands demonstrates their great potential for imaging and optical communications applications.

Open Access Article. Published on 31 May 2024. Downloaded on 6/11/2026 5:03:47 PM.
This article is licensed under a Creative Commons Attribution 3.0 Unported Licence.

Introduction

Luminescent materials continue to attract considerable interest owing to their widespread potential in optical devices and biomedical applications.[1–5] Trivalent lanthanide(III) complexes captured extensive attention in luminescence technology given their unique photoluminescence (PL) characteristics and potential applications in displays,[6] solar cells,[7,8] anti-counterfeiting,[9] luminescent probes for live cell imaging,[10] and sensing.[11] The distinctive PL features of Ln(III) complexes include high color purity (small full width at half maximum), large Stokes shift, and long-lived excited state lifetime due to the Laporte forbidden and intra-configurational nature of f–f transitions.[12] However, the f–f transitions of Ln(III) exhibit very weak absorbance (molar extinction coefficient, $\varepsilon < 10\ M^{-1}\ cm^{-1}$), and thus direct photoexcitation of f–f transition is inefficient. This is known to be overcome by antenna sensitization with suitable organic ligands having high absorption coefficients to exploit the inherent PL features of Ln(III) complexes for various applications.[12,13] Numerous classes of sensitizer ligands have been used for the complexion of Ln(III), however, the choices of ligands are very limited to obtain high energy transfer efficiency.[14–18] For lanthanide complexes, the luminescence quantum efficiency is the product of sensitization efficiency (η_{sens}) and the intrinsic lanthanide emission quantum yield (Φ_{Ln}); ($\Phi_{tot} = \eta_{sens} \times \Phi_{Ln} = \eta_{sens} \times k_r/(k_r + k_{nr})$; k_r and k_{nr} are the radiative and non-radiative decay rate constants, respectively).[19,20] The high Φ_{tot} values in Ln(III) complexes were realized by introducing an asymmetric coordination environment resulting in a large k_r. Anionic β-diketonates are widely used as antennae ligands owing to their stable coordination with Ln(III) cations and large polarizability resulting in large k_r. Rigid neutral ancillary ligands with low vibrational quenching decrease the k_{nr}. Thus Ln(III) complexes with β-diketonate and low vibrational neutral ligands like phosphine oxides are effective for achieving near unity Φ_{tot}.[20] Despite the intriguing luminescent properties and applications of lanthanide complexes, designing chelating antennae/ancillary ligands with large absorption coefficients and stable coordination to Ln(III) ions to develop highly efficient lanthanide emitters is still challenging.

Upon photoexcitation, ligands undergo intersystem crossing (ISC) from the lowest singlet excited state (S_1) to the lowest triplet excited state (T_1), thereby transferring their electronic energy to the Ln(III) ion. Organic ligands with a small singlet (S_1)-triplet (T_1) energy gap (ΔE_{ST}) and longer T_1 lifetime show a high ISC yield. Further, to realize efficient ligand to Ln(III) energy transfer (η_{sens}) and avoid the back energy transfer, the T_1 state of the ligands should lie ~2000–3500 cm^{-1} above the energy-accepting states (EAS) of the Ln(III).[21–24] Expanding the π-conjugation length of ligands leads to a decrease in T_1 energy level, however, in many cases, the limitation arises due to the metal-to-ligand back energy transfer owing to the very small $\Delta E(T_1\text{-EAS})$.[20] Recently Hasegawa and co-workers showed low energy photosensitized emission of Eu(III) complex containing stacked-coronene nanocarbon ligand with a ΔE_{ST} (3700 cm^{-1}) and longer T_1 lifetime (~40 ms) which allows for equilibration (forward and backward energy transfer) between the T_1 state of ligand and EAS state of Eu(III) that led to an emission quantum yield of 61%.[25] A rational design for novel ligands with small ΔE_{ST} and an adequate $\Delta E(T_1\text{-EAS})$ is important in obtaining Ln(III) complexes with efficient energy transfer for improving the luminescence quantum yield.

EaStCHEM School of Chemistry, The University of Edinburgh, Kings Buildings, Edinburgh EH9 3FJ, UK. E-mail: Neil.Robertson@ed.ac.uk

† Electronic supplementary information (ESI) available: [NMR spectra, HRMS, IR, TGA, optical properties and sensitization mechanism are included in the supporting information]. See DOI: https://doi.org/10.1039/d4cp01610f

Open Access Article. Published on 31 May 2024. Downloaded on 6/11/2026 5:03:47 PM.
This article is licensed under a Creative Commons Attribution 3.0 Unported Licence.

Eu(III) coordination polymers with rigid multi-dimensional networks are known to show superior thermal and optical properties ideal for optical devices.[26] Hasegawa and co-workers reported Eu(III) coordination polymers containing hexafluoroacetylacetonate (hfa) and thiophene-based bidentate phosphine oxide bridging ligands with their thermal stability up to ~320 °C and a Φ_{tot} of 60% with 80% η_{sens} in the solid state.[27] A similar Eu(III) coordination polymer containing hfa and furan-based bidentate phosphine oxide bridging ligands exhibited 64% Φ_{tot} with 88% η_{sens} in the solid state.[28] They also reported a highly thermally stable (>300 °C) Eu(III) coordination polymer containing hfa and biphenylene-based bidentate phosphine oxide bridging ligands showing 29% Φ_{tot} with 40% η_{sens} in the solid state.[29] Bünzil and co-workers reported Eu(III) containing hfa and bidentate carboxylic ancillary ligands with a Φ_{Ln} in the range of 77–100%, Φ_{tot} in the range of 18–51% and η_{sens} in the range 23–51% in the solid state.[30]

Our new strategy envisages that ligands with minimal ΔE_{ST} may be constructed with donor–acceptors such that the ligand molecule exhibits thermally activated delayed fluorescence (TADF) properties.[31,32] TADF ligands are then coordinated with lanthanide metals to develop unique new TADF-ligand-anchored Ln(III) β-diketonate complexes. The key point is that the triplet energies of TADF ligands can be easily tuned by facile structural modifications and the ΔE_{ST} of the TADF-sensitizer is only a few hundred cm^{-1}. Subtle molecular design by choosing antennae TADF-ligands having appropriate energy level matching induces intramolecular energy transfer from ligands to Ln(III), enabling highly efficient energy transfer (Fig. 1).

Here we report the synthesis and optical properties of three novel Eu(III) β-diketonates with neutral ancillary TADF-ligands (Scheme 1). The ligands **1L**, **2L**, and **3L** consist of a spiro-(fluorine-9,9′-xanthane) (SFX) unit anchored with weakly electron-accepting diphenylphosphine oxides and diarylamine donors. The S_1 and T_1 energy levels of **1L**, **2L**, and **3L** were fine-tuned by varying the electron-donating strength of diarylamine donors. The design, synthesis, efficient TADF properties, and their application in OLEDs of **1L**, **2L** and **3L** have been reported by us recently.[33] The presence of a diphenylphosphine oxide chelating unit endows them with the ability to coordinate with Ln(III). Promisingly, the excited (S_1 and T_1) state energies of TADF-ligands show optimum energy matching with Eu(III) energy-accepting states. Further, the matching excited state energy levels of theonyltrifluoroacetonate (tta) and the TADF ligands, can accelerate the simultaneous transfer of energy to the Eu(III). Novel Eu(III) coordination polymers **1**, **2**, and **3** containing tta and SFX-based TADF ligands (**1L**, **2L**, and **3L**) were designed, synthesized, and studied for their PL characteristics as a proof of concept of our strategy. The present newly developed Eu-TADF coordination polymers exhibit Eu(III) centered bright red luminescence with a dominant narrow emission band at 611 nm in solution, solid state, and poly-(methyl methacrylate) (PMMA) films. High intrinsic emission quantum yield (~90%) and sensitization efficiency of ~94% were achieved in the TADF ligand-sensitized Eu(III) coordination polymers in PMMA encapsulated films.

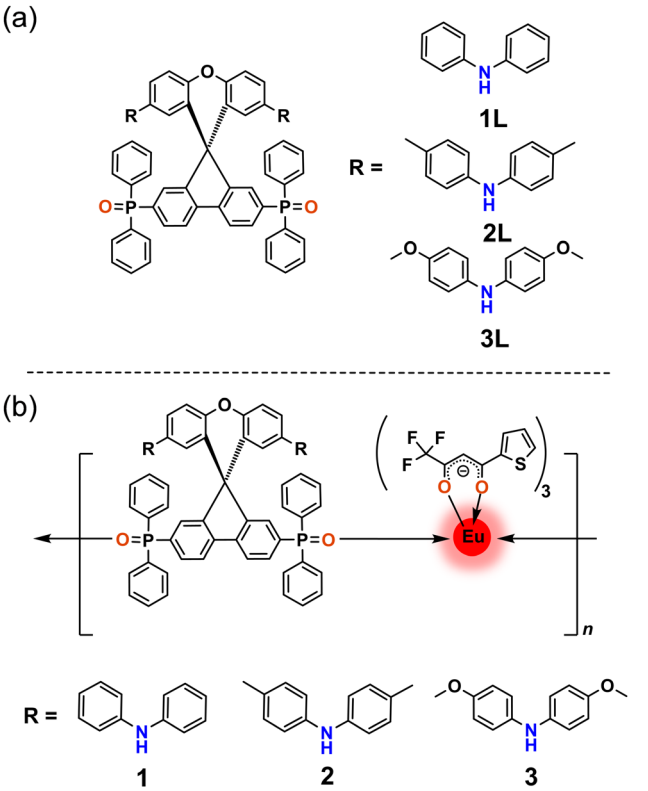

Scheme 1 (a) Chemical structures of TADF-ligands. (b) Chemical structures of Eu(III) coordination polymers with tta and TADF-ligands.

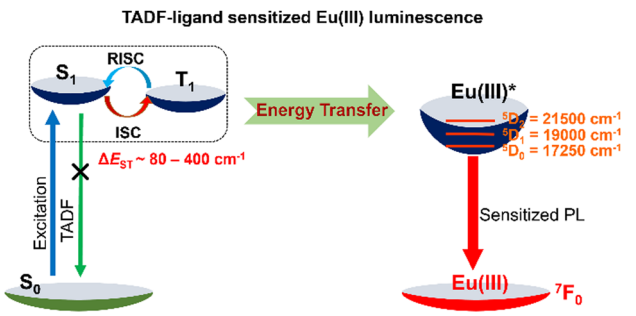

Fig. 1 Strategy for the energy transfer pathway in TADF-ligand sensitized Eu(III) emission.

Experimental section

General methods

All the chemicals were purchased from commercial suppliers (Sigma Aldrich, Fisher Scientific, or Fluorochem, UK) and used as received unless otherwise mentioned. The reactions were performed using standard Schlenk-line techniques under the N_2 atmosphere. NMR spectroscopy was carried out using Bruker Pro500 spectrometers. ^{19}F and ^{31}P NMR spectra were all recorded in deuterated benzene and chemical shifts are reported in parts per million. Mass spectra were recorded with Xevo QTOF (Waters) high resolution, accurate mass tandem

This journal is © the Owner Societies 2024

Open Access Article. Published on 31 May 2024. Downloaded on 6/11/2026 5:03:47 PM. This article is licensed under a Creative Commons Attribution 3.0 Unported Licence.

mass spectrometer equipped with Atmospheric Solids Analysis Probe (ASAP) and Bruker MicroToF 2. All spectra were recorded using electrospray (ESI) ionization. IR spectra were measured at room temperature on a PerkinElmer Spectrum 65 FT-IR spectrometer in a 4000–450 cm^{-1} spectral range. Thermo-Gravimetric Analysis (TGA) curves of compounds were collected in a NETZSCH STA 449 F1 apparatus at a heating rate of 5 °C min^{-1} under a nitrogen atmosphere.

Synthesis

TADF ligands **1L**, **2L** and **3L**[33] and $Eutta_3.2H_2O$[18] were synthesized according to our recently reported procedure. A mixture of $Eutta_3.2H_2O$ (0.05 mmol) and appropriate TADF ligands (0.05 mmol), **1L** for **1**, **2L** for **2**, and **3L** for **3** in HPLC grade acetone was stirred for 2 hours at room temperature and the solvent was evaporated and the compound was dried under vacuum. The resultant residue was recrystallized from a 1 : 1 mixture of acetone and pentane, to get the pure compounds as pale yellow (**1**), yellow (**2**), and dark yellow (**3**) powders in ~95% yield. The complex was characterized by ^{31}P and ^{19}F NMR spectroscopy.

Coordination polymer 1

^{19}F NMR (500 MHz, C_6D_6-d_6): δ (ppm) −79.7; ^{31}P NMR (500 MHz, C_6D_6-d_6): δ (ppm) 76.5. ESI-MS $[M+Na]^+$ calculated ($C_{97}H_{64}Eu_1F_9N_2O_9S_3Na_1$) 1905.2209; found 1905.2223.

Coordination polymer 2

^{19}F NMR (500 MHz, C_6D_6-d_6): δ (ppm) −79.5; ^{31}P NMR (500 MHz, C_6D_6-d_6): δ (ppm) −76.3. ESI-MS $[M+H]^+$ calculated ($C_{101}H_{73}Eu_1F_9N_2O_9P_2S_3$) 1939.3016; found 1939.3030.

Coordination polymer 3

^{19}F NMR (500 MHz, C_6D_6-d_6): δ (ppm) −79.5; ^{31}P NMR (500 MHz, C_6D_6-d_6): δ (ppm) −75.9. ESI-MS $[M+H]^+$ calculated ($C_{101}H_{73}Eu_1F_9N_2O_{13}P_2S_3$) 2003.2813; found 2003.2827.

Photophysical characterization

Optically dilute solutions of compounds were prepared in HPLC grade solvent for UV-Vis absorption and emission analysis. UV-Vis absorption spectra of solution samples were recorded on a Shimadzu UV-1800 double beam spectrophotometer, at room temperature. UV-Vis absorption spectra measurements in diffuse reflectance mode were made on powder samples using a JASCO V-670 spectrophotometer with an integrating sphere attachment. Non-absorbing BaSO4 was used as the reference and the powders were mixed with $BaSO_4$ and were used for the measurements. UV-Vis absorption spectra of PMMA films were also measured on JASCO V-670 spectrophotometer. Steady-state emission and time-resolved emission spectra were recorded with a Fluoromax-P spectrofluorimeter (Horiba–Jobin–Yvon) at 298 K. The concentration of the lanthanide coordination polymers was such as to give an absorbance of around 0.1 at the excitation wavelength, both in solution and polymer matrix. Excitation and emission spectra were measured using the spectrofluorimeter with a continuous xenon lamp excitation source, in photon counting mode. Spectra were corrected for variations in excitation intensity and the response of the detector. Lifetimes were measured using a pulsed xenon lamp source, with pulse width <50 μs, and time-gated detection. Total luminescence quantum yields (Φ_{tot}) of complexes were determined by comparative method solution. Quinine sulphate is used as the standard dye for samples solution state, whose quantum yield (Φ_r) in 1N H_2SO_4 was determined to be 54.6% using the absolute method.[34] Following equation (eqn (1)) was used for the calculation of quantum yield

$$QY_x = QY_r\left(\frac{slope_s}{slope_r}\right)\left(\frac{n_s^2}{n_r^2}\right) \quad (1)$$

Where s and r denote the compound and reference samples, slope is the calculated from the graph of integrated emission *versus* absorbance and n is the refractive index of the solution.

Absolute luminescence quantum yield of solid powders and PMMA encapsulated films were measured using Quanta–Phi (Horiba–Jobin–Yvon) integrating sphere. PMMA films of Eu(III) coordination polymers were prepared by mixing the Eu polymer (2 wt%) and PMMA in toluene followed by spin-casting on a quartz substrate.

Total luminescence quantum yields (Φ_{tot}) of complexes is the product of ligand sensitization efficiency (η_{sens}) and the intrinsic luminescence quantum efficiency of the Ln(III) ion (Φ_{Ln}).[19] Φ_{Ln}, could not be determined experimentally because of the very low intensity of f–f transition, but it can be calculated from the ratio of the lanthanide luminescence lifetime, τ_{Ln}, and its pure radiative lifetime, τ_R. The latter have been calculated from eqn (3), according to method described by Werts *et al.*

$$\Phi_{tot} = \eta_{sens} \times \Phi_{Ln} = \eta_{sens} \times \left(\frac{\tau_{Ln}}{\tau_R}\right) \quad (2)$$

$$\frac{1}{\tau_R} = A_{MD,0} \times n^3 \times \frac{I_{tot}}{I_{MD}} \quad (3)$$

Where η represents the refractive index (an average refractive index of 1.5 was used for solid state measurements) of the medium. $A_{MD,0}$ is the spontaneous emission probability for the $^5D_0/^7F_1$ transition *in vacuo* (14.65 s^{-1}), and I_{tot}/I_{MD} signifies the ratio of the total integrated intensity of the corrected Eu^{3+} emission spectrum to the integrated intensity of the magnetic dipole $^5D_0/^7F_1$ transition.

Further the radiative (k_r) and non-radiative (k_{nr}) decay rate constant were calculated by the following equations (eqn (4) and eqn (5))[20]

$$k_r = \frac{1}{\tau_R} \quad (4)$$

$$k_{nr} = \frac{\tau_R - \tau_{Ln}}{\tau_R \tau_{Ln}} \quad (5)$$

Results and discussion

Synthesis and characterization

The Eu(III) complexes with TADF ligands were synthesized by a modified literature procedure,[18] that involves mixing equimolar amounts of $Eutta_3.2H_2O$ complex with the corresponding TADF

Open Access Article. Published on 31 May 2024. Downloaded on 6/11/2026 5:03:47 PM.
This article is licensed under a Creative Commons Attribution 3.0 Unported Licence.

ligands (**1L** for **1**, **2L** for **2**, and **3L** for **3**) in acetone solution under ambient conditions (Scheme 2). The Eu(III) complexes are stable under ambient conditions and soluble in common organic solvents like toluene, DCM, DCE, $CHCl_3$, and THF. Complexes were characterized by ^{31}P, ^{19}F NMR, ESI-MS, and FT-IR (Fig. S1–S12, ESI†). A shift in the ^{31}P NMR resonance from ~28 ppm of the TADF ligands[33] to ~ −80 ppm in complexes confirms the coordination of P═O with Eu(III), in line with related literature reports[35] (Table S1, ESI†). Further, a shift in the ^{19}F NMR in complexes compared to the free tta ligand also confirms the coordination of tta molecules with Eu(III). ESI-MS showed the molecular ion peak corresponding to the repeating unit in the coordination polymeric structures **1**, **2** and **3**, similar to other Eu(III) coordination polymers reported in literature.[27,28] IR stretching frequencies for P═O were shifted from 1190 cm^{-1} in ligands to 1175 cm^{-1} in complexes and for C═O was shifted from 1645 cm^{-1} in tta to 1610 cm^{-1} in Eu-coordination polymers, clearly pointing to the presence of TADF ligands and tta in the coordination sphere (Fig. S10–S12, ESI†). Several attempts to recrystallize the Eu(III) coordination polymers were unsuccessful. Coordination polymers **1–3** are thermally stable up to 270 °C (Fig. S13, ESI†).

Optical properties

The UV-Vis absorption and PL properties of Eu(III) coordination polymers **1–3** were studied in a toluene solution at room temperature. Coordination polymers **1–3** exhibit absorption profiles including strong peaks at 295, 322, and 340 nm (Fig. S15, ESI†). The ligand tta shows a strong broad absorption around 340 nm. The TADF-ligands **1L**, **2L**, and **3L** exhibited a series of strong absorption bands at 290, 300, and 320 nm. The absorption spectra of Eu(III) coordination polymers are a combined effect of both tta and TADF ligands. The ligand tta shows emission in the region 400–500 nm with maxima around ~450 nm[36] while the TADF ligands show emission in the region 400–700 nm with emission maxima centred around **1L** (~490 nm), **2L** (~492 nm) and **3L** (~514 nm).[33] Since both tta and TADF-ligands show absorption in the same spectral region, both can sensitize Eu(III) simultaneously, upon photoexcitation.

Steady-state PL spectra of polymers in toluene showed the characteristic emission profile of Eu(III),[37] with narrow emission bands (FWHM ~10 nm) corresponding to the $^5D_0$ to ^7F_J (J = 0, 1, 2, 3 and 4) transitions observed around ~578, ~592, ~611, ~650 and ~697 nm (Fig. 2a and S16, λ_{ex} = 340 nm). The very intense, narrow signal around ~611 nm corresponds to the hypersensitive $^5D_0$ to $^7F_2$ transition and is responsible for

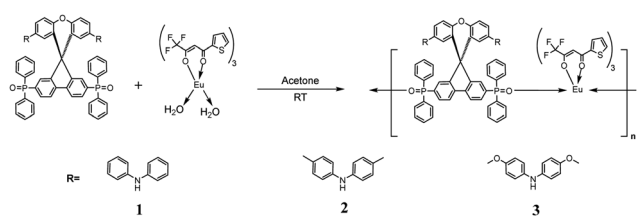

Scheme 2 Synthesis of Eu(III) coordination polymers **1**, **2** and **3**.

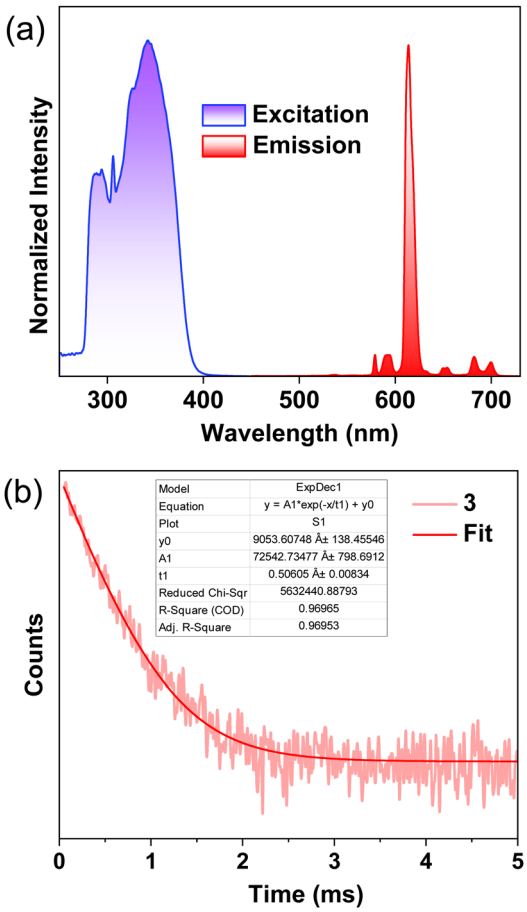

Fig. 2 (a) Excitation and PL spectra and (b) TRPL of **3** in toluene (λ_{ex} = 340 nm and λ_{em}= 611 nm).

the bright red emission colour. The absence of ligand-centred broad emissions (Fig. S14, ESI†) in the PL spectra of complexes, indicates an efficient sensitization of Eu(III) by tta and TADF ligands. The excitation spectral profile collected by monitoring the f–f transitions of complexes matches the absorption spectral profile, evidencing that the excited state energy transfer occurs from TADF and tta ligands to Eu(III). The photosensitization parameters of **1–3** containing TADF ligands are summarized in Table 1 and details about the determination of the optical parameters are described in experimental section. The calculated Φ_{Ln} of the Eu(III) coordination polymers **1–3** are 50, 59, and 45%, and the Φ_{tot} values are determined to be 39, 42, and 29%, respectively in the toluene solution. The excited state energy transfer efficiency (η_{sens}) calculated from the ratio of Φ_{tot} and Φ_{Ln} are 78, 72, and 64%, respectively for **1**, **2**, and **3**. Time-resolved PL (TRPL) decay of **1–3** follows a first-order kinetics with lifetimes in the range of 0.51–0.57 ms (Fig. 2b and Fig. S17, ESI†). The nearly identical k_r ($0.9 \times 10^3 - 1.0 \times 10^3$) and k_{nr} ($7.2 \times 10^2 - 11.0 \times 10^2$) values imply the presence of active non-radiative deactivation pathways that contribute to reduced Φ_{Ln} and Φ_{tot} in solution state.

The optical properties of the coordination polymers were also measured for solid powder samples. The absorption and excitation spectra of Eu(III) polymers in the solid state showed a

This journal is © the Owner Societies 2024

Open Access Article. Published on 31 May 2024. Downloaded on 6/11/2026 5:03:47 PM.
This article is licensed under a Creative Commons Attribution 3.0 Unported Licence.

Table 1 Photophysical properties of **1–3** (λ_{ex} = 340 nm and λ_{em} = 611 nm)

	τ_{Ln}[a] (ms)	τ_R[b] (ms)	Φ_{Ln}[c] (%)	Φ_{tot}[d] (%)	η_{sen}[e] (%)	$k_r \times 10^3$[f] (s^{-1})	$k_{nr} \times 10^3$[g] (s^{-1})
Toluene solution							
1	0.52	1.03	50	39	78	0.98	9.7
2	0.57	0.98	59	42	72	1.00	7.2
3	0.51	1.11	45	29	64	0.90	11.0
Solid powder samples							
1	0.53	0.64	83	56	67	1.6	3.2
2	0.48	0.64	74	59	80	1.6	5.4
3	0.66	0.96	68	57	84	1.0	4.5
PMMA encapsulated films							
1	0.62	0.68	90	85	94	1.5	1.4
2	0.62	0.70	88	79	90	1.4	1.8
3	0.63	0.69	91	84	92	1.4	1.4

[a] Lanthanide luminescence lifetime obtained from TRPL spectra. [b] Radiative lifetime τ_R. [c] The intrinsic luminescence quantum yield $\Phi_{Ln} = \tau_{Ln}/\tau_R$. [d] Total luminescence quantum yields (Φ_{tot}). [e] Sensitization efficiency $\eta_{sen} = \Phi_{tot}/\Phi_{Ln}$. [f] Radiative decay rate constant $k_r = 1/\tau_R$. [g] Non-radiative decay rate constant, $k_{nr} = (\tau_R - \tau_{Ln})/\tau_R\,\tau_{Ln}$.[19,20]

broad absorption band in the region of 280–450 nm (Fig. 3a and Fig. S18, S19, ESI†). Coordination polymers **1–3** showed characteristic Eu(III) centred luminescence similar to that of the solution state. The absence of ligand-centred emission further supports the efficient sensitization of Eu(III) by TADF ligands. A mono-exponential emission decay profile with lifetimes in the range of 0.48–0.66 ms was noted in the solid state (Fig. 3b and Fig. S20, ESI†). Coordination polymers **1**, **2**, and **3** showed high Φ_{Ln} values of 83, 74, and 68%, and Φ_{tot} values are 56, 59, and 57% respectively in the solid state (Fig. S21–23, ESI†). The pure radiative lifetime, τ_R in compound **3** (0.96 ms) is longer compared to **1** (0.64 ms) and **2** (0.64 ms). This could be due to differences in solid state packing; compound **3** may have a less symmetric structure in the solid state and thus an increased rate of radiative f–f transition. Significantly enhanced η_{sens} of ~84% for **3** obtained in the solid state is attributed to the efficient excited state energy transfer accelerated by TADF sensitization (Table 1). Notably, higher values of Φ_{Ln} in the

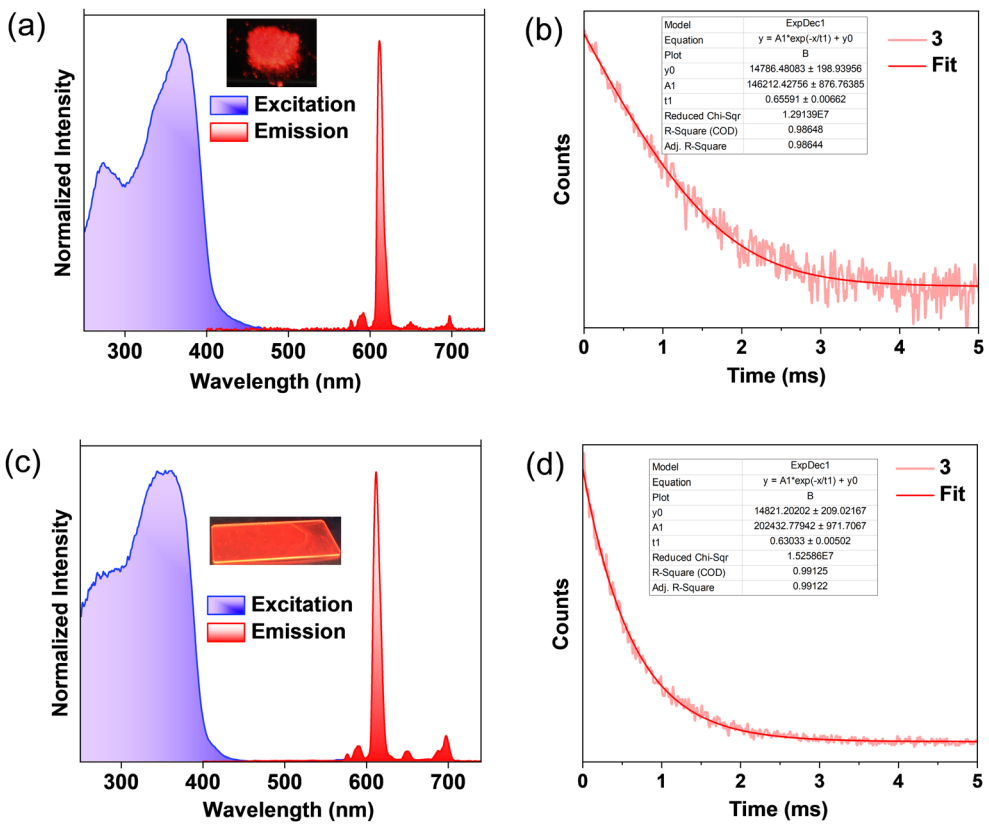

Fig. 3 (a) Excitation and PL spectra of solid powders of **3** and (b) TRPL of solid powders of **3**, (c) excitation and PL spectra of **3** in PMMA encapsulated films and (d) TRPL of **3** in PMMA encapsulated films (λ_{ex} = 340 nm and λ_{em} = 611 nm). The inset shows the images of compound **3** under UV illumination (λ_{ex} = 365 nm).

Open Access Article. Published on 31 May 2024. Downloaded on 6/11/2026 5:03:47 PM.
This article is licensed under a Creative Commons Attribution 3.0 Unported Licence.

solid state compared to the solution state could be due to the suppression of molecular motions, further substantiated by the low k_{nr} values (3.2×10^2 –5.4×10^2).

The PL properties were further measured in PMMA-encapsulated films of polymers **1–3**. The UV-Vis absorption and excitation spectra of 2 wt% PMMA films showed absorption in the region 250–450 nm (Fig. 3c and Fig. S24, S25, ESI†). The PL spectra of **1–3** showed characteristic Eu(III) centered emission and no ligand-centered emissions were observed, further confirming the efficient excited state energy transfer from tta and TADF ligands to Eu(III) upon photoexcitation. The TRPL decay of **1–3** showed a first-order kinetic with a lifetime of 0.62 ms for **1** and **2** and 0.63 ms for **3** (Fig. 3d and Fig. S26, ESI†). In sharp contrast to solid samples, the Φ_{Ln} (~90%) values for 2wt% PMMA films of **1–3** are observed to be higher than for Eu(III) coordination polymers reported.[28–30,38–40] This strategic molecular design further endowed the complexes with a very high Φ_{tot} (~79–85%) due to the remarkably high η_{sens} (~90–94%). Reduced k_{nr} ($1.4–1.8 \times 10^2$) values in films compared to the solution and solid state could be due to suppressed vibrational relaxation and reduced concentration quenching in the polymer matrix that results in high Φ_{Ln}. This high Φ_{tot} and η_{sens} of Eu coordination polymers with TADF ligands point to the potential of this unique molecular design strategy for photonic application.

In the excitation spectra of complexes in PMMA-encapsulated films, a clear tail extends into the visible region, which prompted us to investigate their PL properties under visible excitations. The characteristic Eu(III) centered red emission at 611 nm was observed for a range of excitation wavelength from 300–450 nm for **1–3** (Fig. S30, ESI†). In the visible excitation at 400 nm, the TADF sensitized Eu(III) coordination polymers **1**, **2**, and **3** showed a Φ_{tot} and Φ_{Ln} in the range of 36–39% and 88–91% in PMMA films (Table S2, ESI†). The sensitization efficiency was determined to be in the range of 41–43%. Visible light-sensitized luminescent lanthanide complexes are always demanding for developing less harmful bio-labelling or imaging agents for life sciences.[1,10]

To get more insight into the mechanistic aspects of energy transfer process in these complexes, the excited states (S_1 and T_1) energy level alignment of the ligands, Eu(III) and the possible energy transfer pathways are depicted in Fig. 4 and Fig. S36, S37 (ESI†). The excited state energies of different fragments are used for prediction of the possible sensitization mechanism, while assuming that the absorption is ligand centred and emission is Eu(III) localized. The S_1 and T_1 energy levels of TADF-ligands were experimentally determined from the onset of prompt and delayed emission spectra. The excited state energies of the TADF ligands are, **1L**, S_1 (22 987 cm^{-1}) and T_1 (22 584 cm^{-1}), **2L**, S_1 (22 584 cm^{-1}) and T_1 (22 422 cm^{-1}) and **3L**, S_1 (22 180 cm^{-1}) and T_1 (22 100 cm^{-1}), above their ground (S_0) state. All these ligands showed very small ΔE_{ST} of ~400–80 cm^{-1} (0.05–0.01 eV) owing to the near orthogonal geometry of the donor–acceptor structures, the unique characteristics of TADF molecules.[31] The S_1 and T_1 state energies of the tta ligand are 26 000 cm^{-1} and

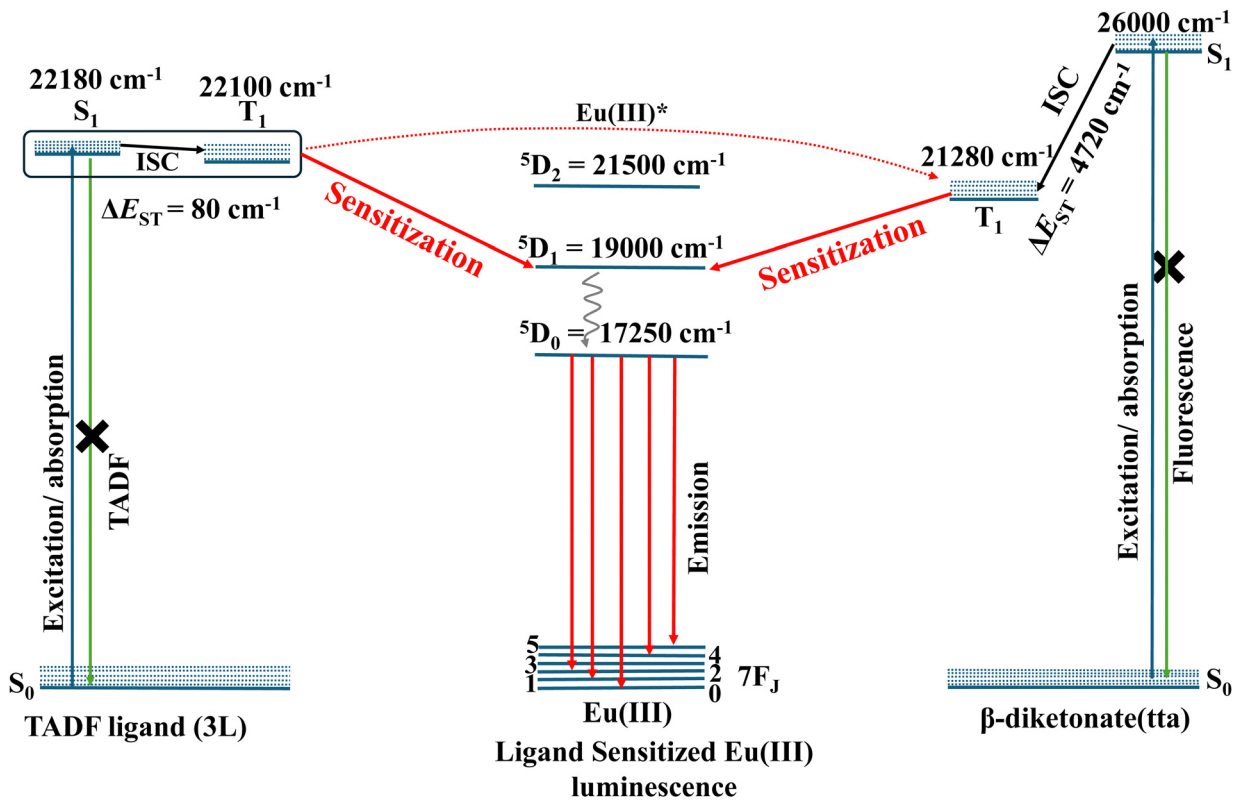

Fig. 4 The mechanistic energy transfer pathways in the tta and TADF-ligand (**3L**) sensitized Eu(III) luminescence of coordination polymer **3** (energy levels are not to the scale).

 This journal is © the Owner Societies 2024

Open Access Article. Published on 31 May 2024. Downloaded on 6/11/2026 5:03:47 PM. This article is licensed under a Creative Commons Attribution 3.0 Unported Licence.

21 280 cm^{-1}, respectively.[21] The excited state energy accepting levels of Eu(III), $^5D_2$, $^5D_1$, and $^5D_0$ lie at 21 500 cm^{-1}, 19 000 cm^{-1}, and 17 250 cm^{-1}, respectively above the $^7F_0$ electronic ground level.[22] The S_1 and T_1 excited states of the ligands have optimum energy to match the energy-accepting states of Eu(III) indicating that TADF ligands can act as efficient photosensitizers for Eu(III). The adequate energy gap between the TADF ligand (**1L**, **2L**, and **3L**) excited states and the Eu(III) excited state promotes the forward energy transfer to the metal and may prevent the backward energy transfer. For instance, as depicted in Fig. 4, the nearly isoenergic S_1 (22 180 cm^{-1}) and T_1 (22 100 cm^{-1}) levels of TADF-ligand **3L** is ~3100 cm^{-1} above the $^5D_1$ state of Eu(III), this adequate energy difference enhances the rate of forward energy transfer, upon photoexcitation in **3**. The T_1 energy level of tta lies ~2280 cm^{-1} above the $^5D_1$ state of Eu(III), another forward energy transfer path to Eu(III) upon photoexcitation. Further, S_1 and T_1 energy levels of **3L** lie in between the S_1 and T_1 energy levels of tta and thus there may be an additional energy transfer from the T_1 excited state of **3L** to the T_1 state of tta and to the Eu(III) excited state, that results in an enhanced rate of excited state energy transfer to Eu and thus high Φ_{tot}.[27,28] The nearly isoenergic S_1 and T_1 energy levels of **1L** (S_1, 22 987 cm^{-1}; T_1, 22 584 cm^{-1}) and **2L** (S_1, 22 584 cm^{-1}; T_1, 22 422 cm^{-1}) lie 3580 cm^{-1} and 3400 cm^{-1}, respectively above the $^5D_1$ state of Eu(III) in coordination polymers **1** and **2**. Adequate energy difference enhances the rate of forward energy transfer, upon photoexcitation (Fig. S36 and S37, ESI†). There may be also an additional energy transfer from the T_1 excited state of **1L** and **2L** to the T_1 state of tta and to the Eu(III) excited state, as S_1 and T_1 energy levels of **1L** and **2L** lies in between the S_1 and T_1 energy levels of tta. Based on the energy level diagram it is clear that the TADF ligands can serve as antennae as well as ancillary ligand for sensitization of Eu(III) (Fig. 4 and Fig. S36, S37, ESI†).

Conclusions

We have demonstrated for the first time that TADF-molecules are efficient photosensitizers for Eu(III). The Eu(III) coordination polymers **1**, **2**, and **3** with TADF ligands showed high luminescence quantum yield (79–85%) and efficient sensitization (90–94%) in PMMA films. The appropriate energy matching criteria of excited state energy levels of TADF ligands and Eu(III) were found to enhance Φ_{Ln} and η_{sens}. Remarkably, efficient photosensitization (75–87%) was realized in the visible light excitation with TADF photosensitizer ligands. This novel approach will also apply to organo-lanthanide emitters in all fields such that our concept has the potential for a broad new sensitizer-ligand paradigm across related fields such as imaging or optical communications.

Conflicts of interest

There are no conflicts to declare.

Acknowledgements

This project is funded by European Union's Horizon 2020 research and innovation programme under the Marie Sklodowska Curie rant agreement H2020-MSCA-IF-2020-101025621 (TADF-LDS). We thank Prof. Anita C. Jones and Dr Iain Wright, School of Chemistry, The University of Edinburgh for support with photoluminescence and Integrating sphere facilities.

Notes and references

1 S. V. Eliseeva and J.-C. G. Bünzli, Lanthanide luminescence for functional materials and bio-sciences, *Chem. Soc. Rev.*, 2010, **39**, 189–227.
2 J. M. Ha, S. H. Hur, A. Pathak, J.-E. Jeong and H. Y. Woo, Recent advances in organic luminescent materials with narrowband emission, *NPG Asia Mater.*, 2021, **13**, 53.
3 Y. Im, M. Kim, Y. J. Cho, J.-A. Seo, K. S. Yook and J. Y. Lee, Molecular Design Strategy of Organic Thermally Activated Delayed Fluorescence Emitters, *Chem. Mater.*, 2017, **29**, 1946–1963.
4 J. Mei, N. L. C. Leung, R. T. K. Kwok, J. W. Y. Lam and B. Z. Tang, Aggregation-Induced Emission: Together We Shine, United We Soar!, *Chem. Rev.*, 2015, **115**, 11718–11940.
5 M. Ji and X. Ma, Recent progress with the application of organic room-temperature phosphorescent materials, *Ind. Chem. Mater.*, 2023, **1**, 582–594.
6 F. Zinna, L. Arrico, T. Funaioli, L. Di Bari, M. Pasini, C. Botta and U. Giovanella, Modular chiral Eu(iii) complexes for efficient circularly polarized OLEDs, *J. Mater. Chem. C*, 2022, **10**, 463–468.
7 R. Datt, S. Bishnoi, H. K. H. Lee, S. Arya, S. Gupta, V. Gupta and W. C. Tsoi, Down-conversion materials for organic solar cells: Progress, challenges, and perspectives, *Aggregate*, 2022, **3**, e185.
8 A. Gavriluta, T. Fix, A. Nonat, A. Slaoui, J.-F. Guillemoles and L. J. Charbonnière, Tuning the chemical properties of europium complexes as downshifting agents for copper indium gallium selenide solar cells, *J. Mater. Chem. A*, 2017, **5**, 14031–14040.
9 J. Andres, R. D. Hersch, J.-E. Moser and A.-S. Chauvin, A New Anti-Counterfeiting Feature Relying on Invisible Luminescent Full Color Images Printed with Lanthanide-Based Inks, *Adv. Funct. Mater.*, 2014, **24**, 5029–5036.
10 M. Cardoso Dos Santos, A. Runser, H. Bartenlian, A. M. Nonat, L. J. Charbonnière, A. S. Klymchenko, N. Hildebrandt and A. Reisch, Lanthanide-Complex-Loaded Polymer Nanoparticles for Background-Free Single-Particle and Live-Cell Imaging, *Chem. Mater.*, 2019, **31**, 4034–4041.
11 J.-C. G. Bünzli and S. V. Eliseeva, Intriguing aspects of lanthanide luminescence, *Chem. Sci.*, 2013, **4**, 1939–1949.
12 J.-C. G. Bünzli and C. Piguet, Taking advantage of luminescent lanthanide ions, *Chem. Soc. Rev.*, 2005, **34**, 1048–1077.
13 Y. Yang, J. Li, X. Liu, S. Zhang, K. Driesen, P. Nockemann and K. Binnemans, Listening to Lanthanide Complexes:

Open Access Article. Published on 31 May 2024. Downloaded on 6/11/2026 5:03:47 PM. This article is licensed under a Creative Commons Attribution 3.0 Unported Licence.

Determination of the Intrinsic Luminescence Quantum Yield by Nonradiative Relaxation, *Chem. Phys. Chem.*, 2008, **9**, 600–606.

14 S. Miyazaki, K. Goushi, Y. Kitagawa, Y. Hasegawa, C. Adachi, K. Miyata and K. Onda, Highly efficient light harvesting of a Eu(III) complex in a host–guest film by triplet sensitization, *Chem. Sci.*, 2023, **14**, 6867–6875.

15 A. S. Kalyakina, V. V. Utochnikova, M. Zimmer, F. Dietrich, A. M. Kaczmarek, R. Van Deun, A. A. Vashchenko, A. S. Goloveshkin, M. Nieger, M. Gerhards, U. Schepers and S. Bräse, Remarkable high efficiency of red emitters using Eu(III) ternary complexes, *Chem. Commun.*, 2018, **54**, 5221–5224.

16 M. S. Khan, R. Ilmi, W. Sun, J. D. L. Dutra, W. F. Oliveira, L. Zhou, W.-Y. Wong and P. R. Raithby, Bright and efficient red emitting electroluminescent devices fabricated from ternary europium complexes, *J. Mater. Chem. C*, 2020, **8**, 5600–5612.

17 R. Ilmi, X. Li, N. K. Al Rasbi, L. Zhou, W.-Y. Wong, P. R. Raithby and M. S. Khan, Two new red-emitting ternary europium(III) complexes with high photoluminescence quantum yields and exceptional performance in OLED devices, *Dalt. Trans.*, 2023, **52**, 12885–12891.

18 O. Moudam, B. C. Rowan, M. Alamiry, P. Richardson, B. S. Richards, A. C. Jones and N. Robertson, Europium complexes with high total photoluminescence quantum yields in solution and in PMMA, *Chem. Commun.*, 2009, 6649–6651.

19 M. H. V. Werts, R. T. F. Jukes and J. W. Verhoeven, The emission spectrum and the radiative lifetime of Eu3+ in luminescent lanthanide complexes, *Phys. Chem. Chem. Phys.*, 2002, **4**, 1542–1548.

20 Y. Kitagawa, M. Tsurui and Y. Hasegawa, Bright red emission with high color purity from Eu(III) complexes with π-conjugated polycyclic aromatic ligands and their sensing applications, *RSC Adv.*, 2022, **12**, 810–821.

21 S. Sato and M. Wada, Relations between Intramolecular Energy Transfer Efficiencies and Triplet State Energies in Rare Earth β-diketone Chelates, *Bull. Chem. Soc. Jpn.*, 1970, **43**, 1955–1962.

22 M. Latva, H. Takalo, V.-M. Mukkala, C. Matachescu, J. C. Rodríguez-Ubis and J. Kankare, Correlation between the lowest triplet state energy level of the ligand and lanthanide(III) luminescence quantum yield, *J. Lumin.*, 1997, **75**, 149–169.

23 M. Pietraszkiewicz, M. Maciejczyk, I. D. W. Samuel and S. Zhang, Highly photo- and electroluminescent 1,3-diketonate Eu(III) complexes with spiro-fluorene-xantphos dioxide ligands: synthesis and properties, *J. Mater. Chem. C*, 2013, **1**, 8028–8032.

24 R. Devi, R. Boddula, J. Tagare, A. B. Kajjam, K. Singh and S. Vaidyanathan, White emissive europium complex with CRI 95%: butterfly vs. triangle structure, *J. Mater. Chem. C*, 2020, **8**, 11715–11726.

25 Y. Kitagawa, F. Suzue, T. Nakanishi, K. Fushimi, T. Seki, H. Ito and Y. Hasegawa, Stacked nanocarbon photosensitizer for efficient blue light excited Eu(III) emission, *Commun. Chem.*, 2020, **3**, 3.

26 Y. Hasegawa, S. Shoji and Y. Kitagawa, Luminescent Eu(III)-based Coordination Polymers for Photonic Materials, *Chem. Lett.*, 2022, **51**, 185–196.

27 Y. Hirai, T. Nakanishi, Y. Kitagawa, K. Fushimi, T. Seki, H. Ito and Y. Hasegawa, Luminescent Europium(III) Coordination Zippers Linked with Thiophene-Based Bridges, *Angew. Chem., Int. Ed.*, 2016, **55**, 12059–12062.

28 Y. Hirai, T. Nakanishi, Y. Kitagawa, K. Fushimi, T. Seki, H. Ito and Y. Hasegawa, Triboluminescence of Lanthanide Coordination Polymers with Face-to-Face Arranged Substituents, *Angew. Chem., Int. Ed.*, 2017, **56**, 7171–7175.

29 K. Miyata, T. Ohba, A. Kobayashi, M. Kato, T. Nakanishi, K. Fushimi and Y. Hasegawa, Thermostable Organo-phosphor: Low-Vibrational Coordination Polymers That Exhibit Different Intermolecular Interactions, *ChemPlusChem*, 2012, **77**, 277–280.

30 S. V. Eliseeva, D. N. Pleshkov, K. A. Lyssenko, L. S. Lepnev, J.-C. G. Bünzli and N. P. Kuzmina, Highly Luminescent and Triboluminescent Coordination Polymers Assembled from Lanthanide β-Diketonates and Aromatic Bidentate O-Donor Ligands, *Inorg. Chem.*, 2010, **49**, 9300–9311.

31 H. Nakanotani, T. Higuchi, T. Furukawa, K. Masui, K. Morimoto, M. Numata, H. Tanaka, Y. Sagara, T. Yasuda and C. Adachi, High-efficiency organic light-emitting diodes with fluorescent emitters, *Nat. Commun.*, 2014, **5**, 4016.

32 M. Y. Wong and E. Zysman-Colman, Purely Organic Thermally Activated Delayed Fluorescence Materials for Organic Light-Emitting Diodes, *Adv. Mater.*, 2017, **29**, 1605444.

33 N. Sharma, M. Maciejczyk, D. Hall, W. Li, V. Liégeois, D. Beljonne, Y. Olivier, N. Robertson, I. D. W. Samuel and E. Zysman-Colman, Spiro-Based Thermally Activated Delayed Fluorescence Emitters with Reduced Nonradiative Decay for High-Quantum-Efficiency, Low-Roll-Off, Organic Light-Emitting Diodes, *ACS Appl. Mater. Interfaces*, 2021, **13**, 44628–44640.

34 W. H. Melhuish, Quantum efficiencies of fluorescence of organic substances: Effect of solvent and concentration efficiencies of fluorescent solute1, *J. Phys. Chem.*, 1961, **65**, 229–235.

35 V. Divya, R. O. Freire and M. L. P. Reddy, Tuning of the excitation wavelength from UV to visible region in Eu^{3+} -β-diketonate complexes: Comparison of theoretical and experimental photophysical properties, *Dalton. Trans.*, 2011, **40**, 3257–3268.

36 H. Xu, L.-H. Wang, X.-H. Zhu, K. Yin, G.-Y. Zhong, X.-Y. Hou and W. Huang, Application of Chelate Phosphine Oxide Ligand in Eu Complex with Mezzo Triplet Energy Level, Highly Efficient Photoluminescent, and Electroluminescent Performances, *J. Phys. Chem. B*, 2006, **110**, 3023–3029.

37 K. Binnemans, Interpretation of europium(III) spectra, *Coord. Chem. Rev.*, 2015, **295**, 1–45.

38 V. Jornet-Mollá, C. Dreessen and F. M. Romero, Robust Lanthanoid Picolinate-Based Coordination Polymers for Luminescence and Sensing Applications, *Inorg. Chem.*, 2021, **60**, 10572–10584.

 This journal is © the Owner Societies 2024

39 Y. Hasegawa, S. Tateno, M. Yamamoto, T. Nakanishi, Y. Kitagawa, T. Seki, H. Ito and K. Fushimi, Effective Photo- and Triboluminescent Europium(III) Coordination Polymers with Rigid Triangular Spacer Ligands, *Chem. – Eur. J.*, 2017, **23**, 2666–2672.

40 N. Koiso, Y. Kitagawa, T. Nakanishi, K. Fushimi and Y. Hasegawa, Eu(III) Chiral Coordination Polymer with a Structural Transformation System, *Inorg. Chem.*, 2017, **56**, 5741–5747.

Open Access Article. Published on 31 May 2024. Downloaded on 6/11/2026 5:03:47 PM.
This article is licensed under a Creative Commons Attribution 3.0 Unported Licence.